**Speciation, distribution, and mobility of hazardous trace elements in coal fly ash: Insights from Cr, Ni, and Cu**

Pan Liu, Qian Wang, Haesung Jung, Yuanzhi Tang*

School of Earth and Atmospheric Sciences, Georgia Institute of Technology, 311 Ferst Dr, Atlanta, GA 30332-0340, USA

* Corresponding author.

Email: yuanzhi.tang@eas.gatech.edu; Phone: 404-894-3814

13 total pages

5 tables

5 figures

**Table S1.** Details of Cr, Ni, and Cu reference compounds used in this study.

| **Cr** | **Oxidation state** | **Source or preparation method** |
|---|---|---|
| $FeCr_2O_4$ | +3 | Spectrum from (Tang et al., 2007) |
| $Ca_3Cr_2(SiO_4)_3$ | +3 | Spectrum from (Tang et al., 2007) |
| $Cr_2O_3$ | +3 | Spectrum from (Tang et al., 2007) |
| Cr(III)-doped $Fe_2O_3$ | +3 | $CrCl_3$ were added with equivalent 2% Cr during hematite synthesis following method in (Cornell and Schwertmann, 2003) |
| Cr(III)-doped glass | +3 | 100-µM $CrCl_3$ were added during glass synthesis following method in (De Witte and Uytterhoeven, 1996) |
| $CaCrO_4$ | +6 | Spectrum from (Tang et al., 2007) |
| **Ni** | **Oxidation state** | **Source or preparation method** |
| NiO | +2 | Spectrum from (McNear Jr et al., 2007) |
| $Ni_3(PO_4)_2$ | +2 | Spectrum from (McNear Jr et al., 2007) |
| $NiFe_2O_4$ | +2 | Spectrum from (McNear Jr et al., 2007) |
| Ni(II)-doped $Fe_2O_3$ | +2 | $Ni(NO_3)_2$ were added with equivalent 2% Ni during hematite synthesis following method in (Cornell and Schwertmann, 2003) |
| Ni(II)-doped glass | +2 | 100-µM $Ni(NO_3)_2$ were added during glass synthesis following method in (De Witte and Uytterhoeven, 1996) |
| **Cu** | **Oxidation state** | **Source or preparation method** |
| $Cu_2O$ | +1 | Purchased from Sigma Aldrich |
| CuO | +2 | Spectrum from (Zeng et al., 2018) |
| Cu(II) doped $Fe_2O_3$ | +2 | $CuSO_4$ were added with equivalent 2% Cu during hematite synthesis following method in (Cornell and Schwertmann, 2003) |
| Cu(II)-doped glass | +2 | 100-µM $CuSO_4$ were added during glass synthesis following method in (De Witte and Uytterhoeven, 1996) |

**Table S2.** Mineralogical compositions of CFA samples determined using Rietveld method from (Winburn et al., 2000).

| **Sample F-2** | | **Sample C-2** | |
|---|---|---|---|
| **Phase** | **Percentage (wt%)** | **Phase** | **Percentage (wt%)** |
| glass | 77.4 | glass | 66.3 |
| quartz, $SiO_2$ | 12.6 | tricalcium aluminate, $Ca_3Al_2O_6$ | 4.3 |
| mullite, $Al_6Si_2O_{13}$ | 8.8 | anhydrite, $CaSO_4$ | 2.7 |
| hematite, $Fe_2O_3$ | 0.6 | periclase, MgO | 2.3 |
| magnetite, $Fe_3O_4$ | 0.6 | quartz, $SiO_2$ | 2.3 |
| | | hematite, $Fe_2O_3$ | 1.5 |
| | | lime, CaO | 0.7 |
| | | mullite, $Al_6Si_2O_{13}$ | 0.7 |

**Table S3**. Summary of SEM-EDX results on the speciation and distribution of Cr, Ni, and Cu.

| Figure# | Sample | Particle size (μm) | Chemical composition by EDX | Particle association |
|---|---|---|---|---|
| Fig. 1a | F-2 | ~5 | Cr (moderate*) co-localized with Fe (moderate), Al (low), and Mg (low) | Discrete particle |
| Fig. 1b | C-1 | ~10 | Cr (very low) co-localized with Fe (very high), Al (very low), and Ca (very low) | Encapsulated in glass phase |
| Fig. 1c | C-2 | ~15 | Cr (very low) co-localized with Si (high), Fe (low), Ca (low), and Ni (very low) | On the edge of a quartz particle |
| Fig. S3a | F-2 | ~15 | Cr (low) co-localized with Fe (high) and Ni (low) | Discrete particle |
| Fig. S3b | F-1 | ~3 | Cr (low) co-localized with Fe (high), Ca (low), and Ni (low) | Encapsulated in glass phase |
| Fig. S3c | F-2 | ~2 | Cr (very low) co-localized with Fe (high), Na (low), Si (low), and Al (low) | Encapsulated in glass phase |
| Fig. S4a | F-1 | ~5 | Cr (very low) co-localized with Si (moderate), Al (low), Ca (low), and Fe (low) | Encapsulated in glass phase |
| Fig. S4b | C-2 | ~5 | Cr (very low) co-localized with Ca (high), Si (low), Al (low), Fe (very low), and Zn (very low) | Encapsulated in glass phase |
| Fig. 2a | F-2 | ~15 | Ni (high) co-localized with P (low), Si (low), and Al (low) | Ni likely coating on an unburnt carbon particle and encapsulated in glass phase |
| Fig. 2b | C-2 | ~15 | Ni (high) co-localized with C, P (low), Si (low), and Al (low) | Ni likely coating on an unburnt carbon particle and encapsulated in glass phase |
| Fig. 2c | C-2 | ~15 | Ni (very high) co-localized with P (low) | Encapsulated in glass phase |
| Fig. S5a | C-2 | ~10 | Ni (high) co-localized with P (low), Al (low), and Ca (low) | Discrete particle |
| Fig. S5b | C-2 | ~5 | Ni (very high) co-localized with Al (low) and Si (low) | Encapsulated in glass phase |
| Fig. S5c | F-2 | ~2 | Ni (moderate), the presence of Si (high) and Al (low) is likely due to the proximity to glass phase | Encapsulated in glass phase |
| Fig. 3a | F-1 | ~8 | Cu (moderate) co-localized with Zn (low), the presence of Si (low), Al (low), and Ca (low) is likely due to the proximity to glass phase | Encapsulated in glass phase |
| Fig. 3b | F-2 | ~5 | Cu (very low) co-localized with Fe (moderate) and Cr (very low), the presence of Si (moderate) and Al (low) is likely due to proximity to glass phase | Encapsulated in glass phase |

*Element abundance are labeled based on their oxide content (wt%) detected by EDX: very high >75%, high >50%, moderate >25%, low >5%, very low <5%.

**Table S4.** Summary of the sequential extraction results of CFA samples.

| Element / Parameter | | Class F CFA | | Class C CFA | |
|---|---|---|---|---|---|
| | | F-1 | F-2 | C-1 | C-2 |
| Cr | Total content (ppm) | 174.6 | 59.2 | 85.9 | 67.9 |
| | Water/acid soluble, exchangeable (%) | 10.6 | 7.2 | 33.5 | 48.1 |
| | Reducible (%) | 14.3 | 21.8 | 37.9 | 30.0 |
| | Oxidizable (%) | 2.3 | 5.2 | 4.8 | 6.6 |
| | Residue (%) | 72.8 | 65.8 | 23.8 | 15.3 |
| | Mobile fraction (%)* | 27.2 | 34.2 | 76.2 | 84.7 |
| | Mobile fraction amount (mg/Kg CFA or ppm) | 47.5 | 20.2 | 65.5 | 57.5 |
| | Risk assessment code** | medium | low | high | high |
| Mn | Total content (ppm) | 148.3 | 155.4 | 207.4 | 153.3 |
| | Water/acid soluble, exchangeable (%) | 13.5 | 4.0 | 30.6 | 28.9 |
| | Reducible (%) | 18.6 | 36.1 | 58.8 | 40.8 |
| | Oxidizable (%) | 2.4 | 2.6 | 2.8 | 8.6 |
| | Residue (%) | 65.5 | 57.3 | 7.8 | 21.7 |
| | Mobile fraction (%) | 34.5 | 42.7 | 92.2 | 78.3 |
| | Mobile fraction amount (mg/Kg CFA or ppm) | 51.2 | 66.4 | 191.2 | 120.0 |
| | Risk assessment code | medium | low | high | medium |
| Co | Total content (ppm) | 45.1 | 14.9 | 23.1 | 28.4 |
| | Water/acid soluble, exchangeable (%) | 2.0 | 2.3 | 32.3 | 30.0 |
| | Reducible (%) | 9.0 | 18.5 | 41.0 | 23.5 |
| | Oxidizable (%) | 1.9 | 1.6 | 1.7 | 8.1 |
| | Residue (%) | 87.1 | 77.6 | 25.0 | 38.4 |
| | Mobile fraction (%) | 12.9 | 22.4 | 75.0 | 61.6 |
| | Mobile fraction amount (mg/Kg CFA or ppm) | 5.8 | 3.3 | 17.3 | 17.5 |
| | Risk assessment code | low | low | high | high |
| Ni | Total content (ppm) | 116.8 | 42.2 | 57.0 | 59.4 |
| | Water/acid soluble, exchangeable (%) | 2.8 | 1.9 | 37.9 | 37.5 |
| | Reducible (%) | 7.1 | 14.3 | 31.9 | 19.6 |
| | Oxidizable (%) | 1.7 | 1.0 | 1.3 | 10.7 |
| | Residue (%) | 88.4 | 82.8 | 28.9 | 32.2 |
| | Mobile fraction (%) | 11.6 | 17.2 | 71.1 | 67.8 |
| | Mobile fraction amount (mg/Kg CFA or ppm) | 13.5 | 7.3 | 40.5 | 40.3 |
| | Risk assessment code | low | low | high | high |
| Cu | Total content (ppm) | 128.3 | 66.8 | 183.5 | 180.7 |
| | Water/acid soluble, exchangeable (%) | 14.0 | 31.2 | 34.4 | 38.3 |
| | Reducible (%) | 17.3 | 14.3 | 45.5 | 31.6 |
| | Oxidizable (%) | 4.6 | 7.1 | 3.7 | 11.4 |
| | Residue (%) | 64.1 | 47.4 | 16.4 | 18.7 |
| | Mobile fraction (%) | 35.9 | 52.6 | 83.6 | 81.3 |
| | Mobile fraction amount (mg/Kg CFA or ppm) | 46.1 | 35.1 | 153.4 | 146.9 |
| | Risk assessment code | medium | high | high | high |
| Zn | Total content (ppm) | 169.9 | 92.2 | 109.4 | 120.2 |
| | Water/acid soluble, exchangeable (%) | 4.5 | 5.1 | 29.8 | 31.0 |
| | Reducible (%) | 20.9 | 37.0 | 52.6 | 35.5 |
| | Oxidizable (%) | 6.1 | 14.4 | 9.1 | 16.1 |
| | Residue (%) | 68.5 | 43.5 | 8.5 | 17.4 |
| | Mobile fraction (%) | 31.5 | 56.5 | 81.5 | 82.6 |
| | Mobile fraction amount (mg/Kg CFA or ppm) | 53.5 | 52.1 | 100.1 | 99.3 |
| | Risk assessment code | low | low | medium | high |
| Cd | Total content (ppm) | 48.1 | 39.0 | 43.1 | 54.1 |
| | Water/acid soluble, exchangeable (%) | 2.3 | 1.6 | 13.3 | 14.0 |
| | Reducible (%) | 3.6 | 9.4 | 23.3 | 14.9 |
| | Oxidizable (%) | 1.1 | 2.1 | 2.0 | 13.9 |
| | Residue (%) | 93.0 | 86.9 | 61.4 | 57.2 |
| | Mobile fraction (%) | 7.0 | 13.1 | 38.6 | 42.8 |
| | Mobile fraction amount (mg/Kg CFA or ppm) | 3.4 | 5.1 | 16.6 | 23.2 |
| | Risk assessment code | low | low | medium | medium |
| Pb | Total content (ppm) | 84.4 | 33.6 | 40.5 | 35.5 |
| | Water/acid soluble, exchangeable (%) | 2.4 | 2.6 | 10.6 | 12.7 |
| | Reducible (%) | 2.1 | 5.5 | 8.5 | 7.6 |
| | Oxidizable (%) | 2.1 | 2.0 | 15.8 | 27.7 |
| | Residue (%) | 93.4 | 89.9 | 65.1 | 52.0 |
| | Mobile fraction (%) | 6.6 | 10.1 | 34.9 | 48.0 |
| | Mobile fraction amount (mg/Kg CFA or ppm) | 5.6 | 3.4 | 14.1 | 17.0 |
| | Risk assessment code | low | low | medium | medium |

* Mobile fraction is the sum of water/acid-soluble and exchangeable, reducible, and oxidizable fractions.

****** Risk assessment code (RAC): based on the water/acid soluble and exchangeable fraction (%), there are five risk levels: no risk for <1%, low risk for 1–10%, medium risk for 10–30%, high risk for 30–50%, and very high risk for >50% (Saqib and Bäckström, 2016; Yan et al., 2010; Zhao et al., 2018).

**Table S5.** Summary of sequential extraction results of trace elements in CFA samples from the U.S. and other countries.

| | Reference | This study and Ref. 1 | | Ref. 2 | Ref. 3 | This study and Ref. 1 | | Ref. 3 | Ref. 4 | Ref. 5 | Ref. 6 | Ref. 7 | Ref. 8 | Ref. 9 | | Ref. 10 | | |
|---|---|---|---|---|---|---|---|---|---|---|---|---|---|---|---|---|---|---|
| | Sample source | U.S. | U.S. | U.S. | U.S. | U.S. | U.S. | U.S. | China | China | China | Brazil | U.S. | Poland | Slovakia | China | Japan | Indonesia |
| | CFA type | F | F | F | F | C | C | C | F | F | F(?) | F | F | F | F | F | F | F |
| | # of samples | 1 | 1 | 1 | 6 | 1 | 1 | 2 | 3 | 2 | 2 | 1 | 1 | 1 | 1 | 8 | 1 | 1 |
| **Cr** | Water/acid soluble, exchangeable (%) | 10.6 | 7.2 | | | 33.5 | 48.1 | | 4.6 | | ~10 | ~15 | 4.2 | 18 | 12 | ~10 | ~5 | ~10 |
| | Reducible (%) | 14.3 | 21.8 | | | 37.9 | 30.0 | | 13.1 | | ~1 | ~10 | 11.5 | 5 | 6 | ~5 | ~5 | ~10 |
| | Oxidizable (%) | 2.3 | 5.2 | | | 4.8 | 6.6 | | 2.9 | | ~4 | ~15 | 26.9 | 9 | 8 | ~5 | ~5 | ~10 |
| | Residue (%) | 72.8 | 65.8 | | | 23.8 | 15.3 | | 79.5 | | ~85 | ~60 | 57.3 | 68 | 74 | ~80 | ~85 | ~70 |
| **Mn** | Water/acid soluble, exchangeable (%) | 13.5 | 4.0 | 15.9 | ~5 | 30.6 | 28.9 | ~10 | | | | ~50 | | 6.1 | 8 | | | |
| | Reducible (%) | 18.6 | 36.1 | 10.8 | ~5 | 58.8 | 40.8 | ~15 | | | | ~10 | | 6 | 3 | | | |
| | Oxidizable (%) | 2.4 | 2.6 | 5.9 | ~2 | 2.8 | 8.6 | ~30 | | | | ~5 | | 4 | 2 | | | |
| | Residue (%) | 65.5 | 57.3 | 67.3 | >85 | 7.8 | 21.7 | ~45 | | | | ~25 | | 84 | 87 | | | |
| **Co** | Water/acid soluble, exchangeable (%) | 2.0 | 7.1 | | | 33.3 | 30.0 | | | | ~10 | | | | | | | |
| | Reducible (%) | 9.0 | 18.5 | | | 41.0 | 23.5 | | | | ~1 | | | | | | | |
| | Oxidizable (%) | 1.9 | 1.6 | | | 1.7 | 8.1 | | | | ~2 | | | | | | | |
| | Residue (%) | 87.1 | 77.6 | | | 25.0 | 38.4 | | | | ~85 | | | | | | | |
| **Ni** | Water/acid soluble, exchangeable (%) | 2.8 | 1.9 | | | 37.9 | 37.5 | | | | ~15 | | | 5.2 | 7.4 | | | |
| | Reducible (%) | 7.1 | 14.3 | | | 31.9 | 19.6 | | | | ~1 | | | 2 | 3 | | | |
| | Oxidizable (%) | 1.7 | 1.0 | | | 1.3 | 10.7 | | | | ~4 | | | 1 | 1 | | | |
| | Residue (%) | 88.4 | 82.8 | | | 28.9 | 32.2 | | | | ~80 | | | 92 | 89 | | | |
| **Cu** | Water/acid soluble, exchangeable (%) | 14.0 | 31.2 | | | 34.4 | 38.3 | | 17.3 | | ~20 | ~10 | 9.7 | 10.1 | 9.1 | | | |
| | Reducible (%) | 17.3 | 14.3 | | | 45.5 | 31.6 | | 25 | | ~10 | ~10 | 5.0 | 4 | 2 | | | |
| | Oxidizable (%) | 4.6 | 7.1 | | | 3.7 | 11.4 | | 4.4 | | ~10 | ~15 | 17.3 | 1 | 2 | | | |
| | Residue (%) | 64.1 | 47.4 | | | 16.4 | 18.7 | | 53.3 | | ~60 | ~65 | 68.0 | 85 | 87 | | | |
| **Zn** | Water/acid soluble, exchangeable (%) | 4.5 | 5.1 | | | 29.8 | 31.0 | | 17.2 | | ~15 | ~12 | 1 | 4 | 4 | | | |
| | Reducible (%) | 20.9 | 37.0 | | | 52.6 | 35.5 | | 18.1 | | ~2 | ~5 | 14.2 | 2 | 1 | | | |
| | Oxidizable (%) | 6.1 | 14.4 | | | 9.1 | 16.1 | | 4.1 | | ~3 | ~13 | 13.9 | 0.3 | 1 | | | |
| | Residue (%) | 68.5 | 43.5 | | | 8.5 | 17.4 | | 60.5 | | ~80 | ~70 | 70.9 | 94 | 94 | | | |
| **Cd** | Water/acid soluble, exchangeable (%) | 2.3 | 1.6 | | | 13.3 | 14.0 | | | | ~25 | ~0 | | | | | | |
| | Reducible (%) | 3.6 | 9.4 | | | 23.3 | 14.9 | | | | ~2 | ~0 | | | | | | |
| | Oxidizable (%) | 1.1 | 2.1 | | | 2.0 | 13.9 | | | | ~3 | ~0 | | | | | | |
| | Residue (%) | 93.0 | 86.9 | | | 61.4 | 57.2 | | | | ~70 | ~100 | | | | | | |
| **Pb** | Water/acid soluble, exchangeable (%) | 2.4 | 2.6 | | | 10.6 | 12.7 | | 1.1 | | ~1 | ~0 | 4.3 | | | | | |
| | Reducible (%) | 2.1 | 5.5 | | | 8.5 | 7.6 | | 16.4 | | ~1 | ~10 | 4.4 | | | | | |
| | Oxidizable (%) | 2.1 | 2.0 | | | 15.8 | 27.7 | | 4.9 | | ~1 | ~15 | 16.5 | | | | | |
| | Residue (%) | 93.4 | 89.9 | | | 65.1 | 52.0 | | 83.9 | | ~97 | ~75 | 74.7 | | | | | |
| **REE** | Water/acid soluble, exchangeable (%) | ~3 | ~5 | 5.2 | ~5 | ~25 | ~35 | ~10 | | ~10 | | | | | | | | |
| | Reducible (%) | ~15 | ~30 | 0.6 | ~5 | ~55 | ~45 | ~15 | | ~3 | | | | | | | | |
| | Oxidizable (%) | ~2 | ~5 | 8.3 | ~2 | ~5 | ~5 | ~30 | | ~17 | | | | | | | | |
| | Residue (%) | ~80 | ~60 | 86.1 | >85 | ~15 | ~15 | ~45 | | ~80 | | | | | | | | |

Ref. 1 (Liu et al., 2019); Ref. 2 (Lin et al., 2018); Ref. 3 (Taggart et al., 2018); Ref. 4 (Fu et al., 2019); Ref. 5 (Pan et al., 2019); Ref. 6 (Yuan, 2009); Ref. 7 (Quispe et al., 2012); Ref. 8 (Jegadeesan et al., 2008); (Smeda and Zyrnicki, 2002); Ref. 9 (Smeda and Zyrnicki, 2002); Ref. 10 (Tian et al., 2018)

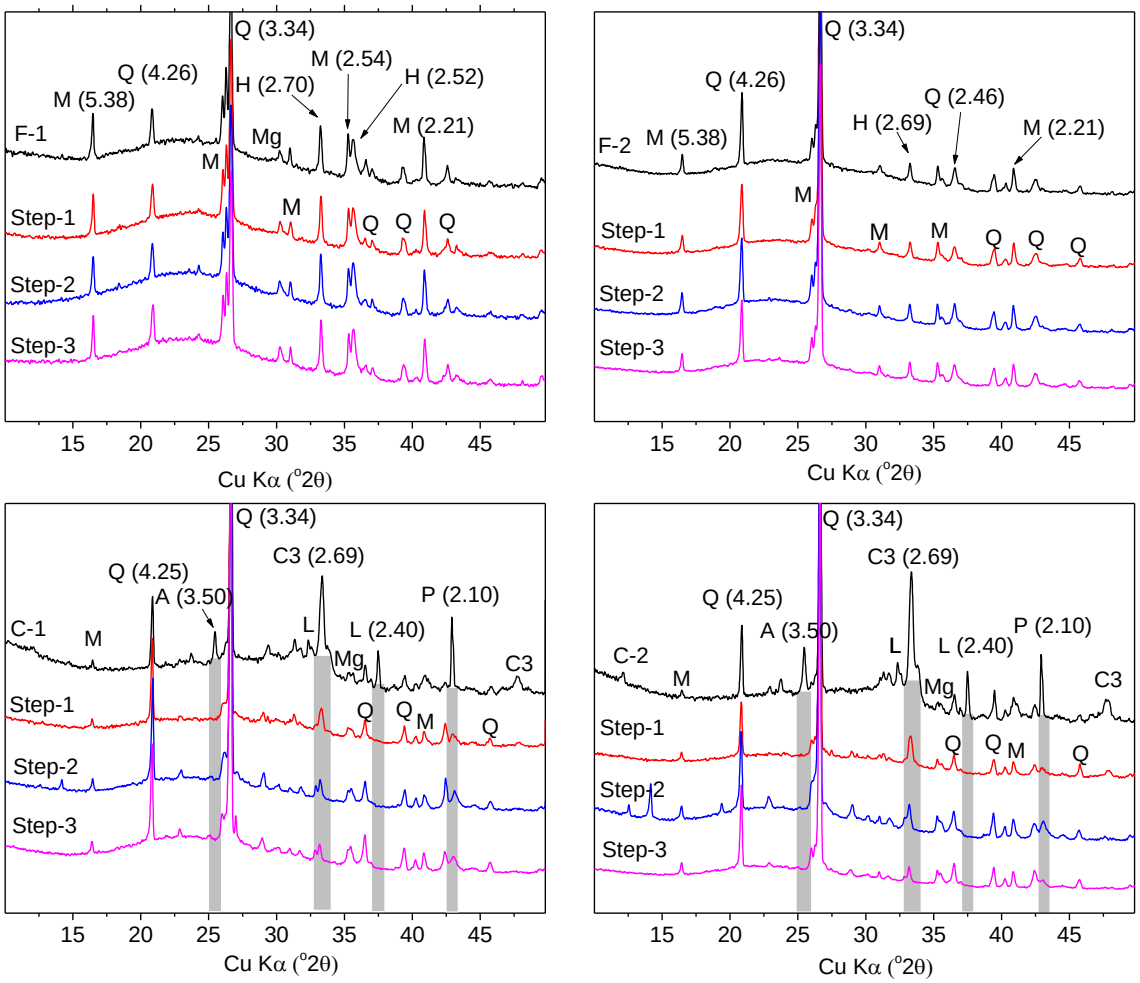


**Figure S1.** X-ray diffraction (XRD) patterns of CFA samples before and after each sequential chemical extraction step. Q (quartz), M (mullite), A (anhydrite), P (periclase), L (lime), C3 (tricalcium aluminate), Mg (magnetite), H (hematite). Numbers in the parentheses denote the d-spacing values (Å) of main reflection peaks. Vertical gray shadings indicate the main mineral phases that dissolved during the sequential extraction steps. Step-1, Step-2, and Step-3 refer to the residues after extraction of (1) Step-1: water-soluble/exchangeable/acid-soluble (e.g., carbonates), (2) Step-2: reducible (e.g., Fe-Mn oxides), and (3) Step-3: oxidizable (e.g., organic matter and sulfide) fractions in CFA samples. The XRD patterns were collected using a Panalytical Empyrean diffractometer and presented in the SI of (Liu et al., 2019).

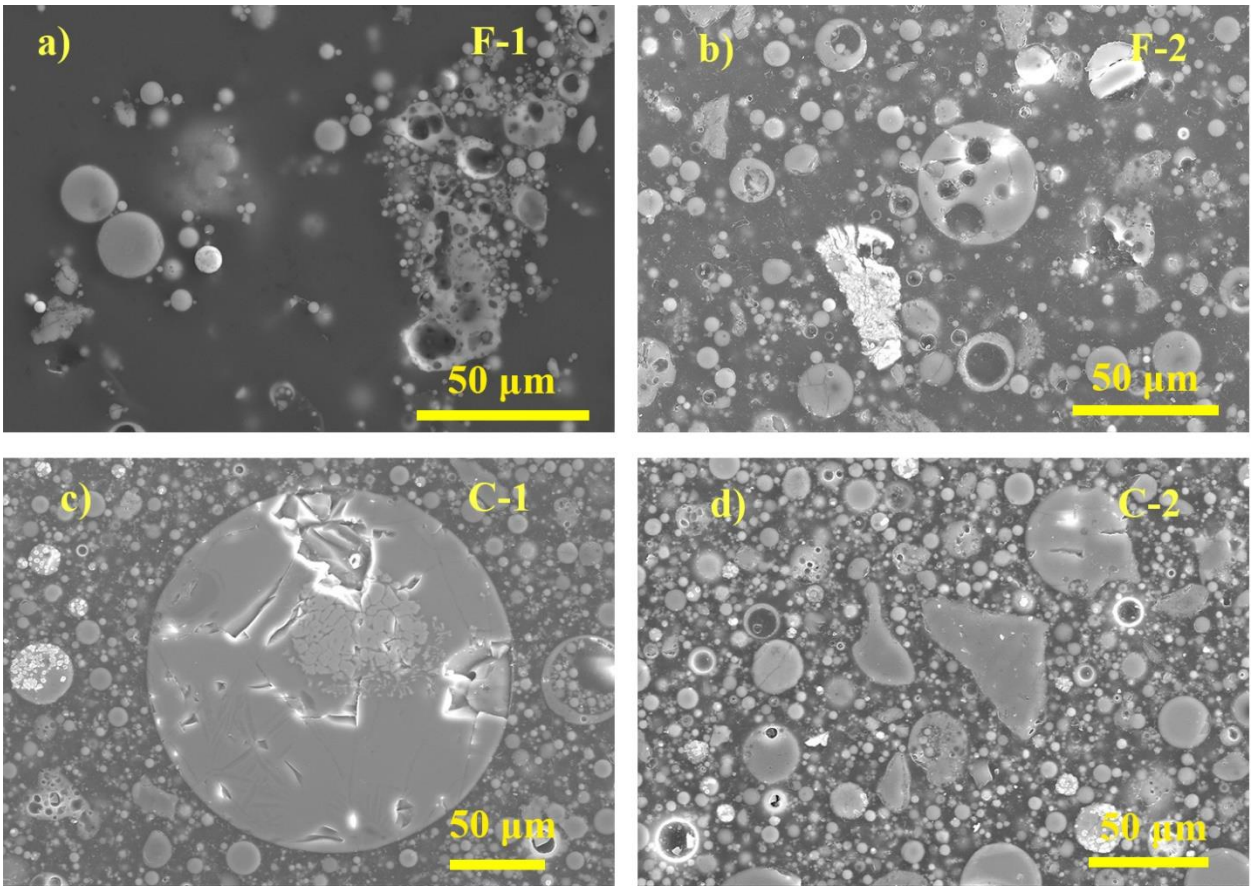


**Figure S2**. Representative SEM images of CFA samples (a) F-1, (b) F-2, (c) C-1, and (d) C-2. Note the common presence of spheres, cenospheres (particles with an empty hollow core), or plerospheres (particles with a hollow core that is filled with other particles). SEM image of C-2 has been presented in the SI of (Liu et al., 2019).

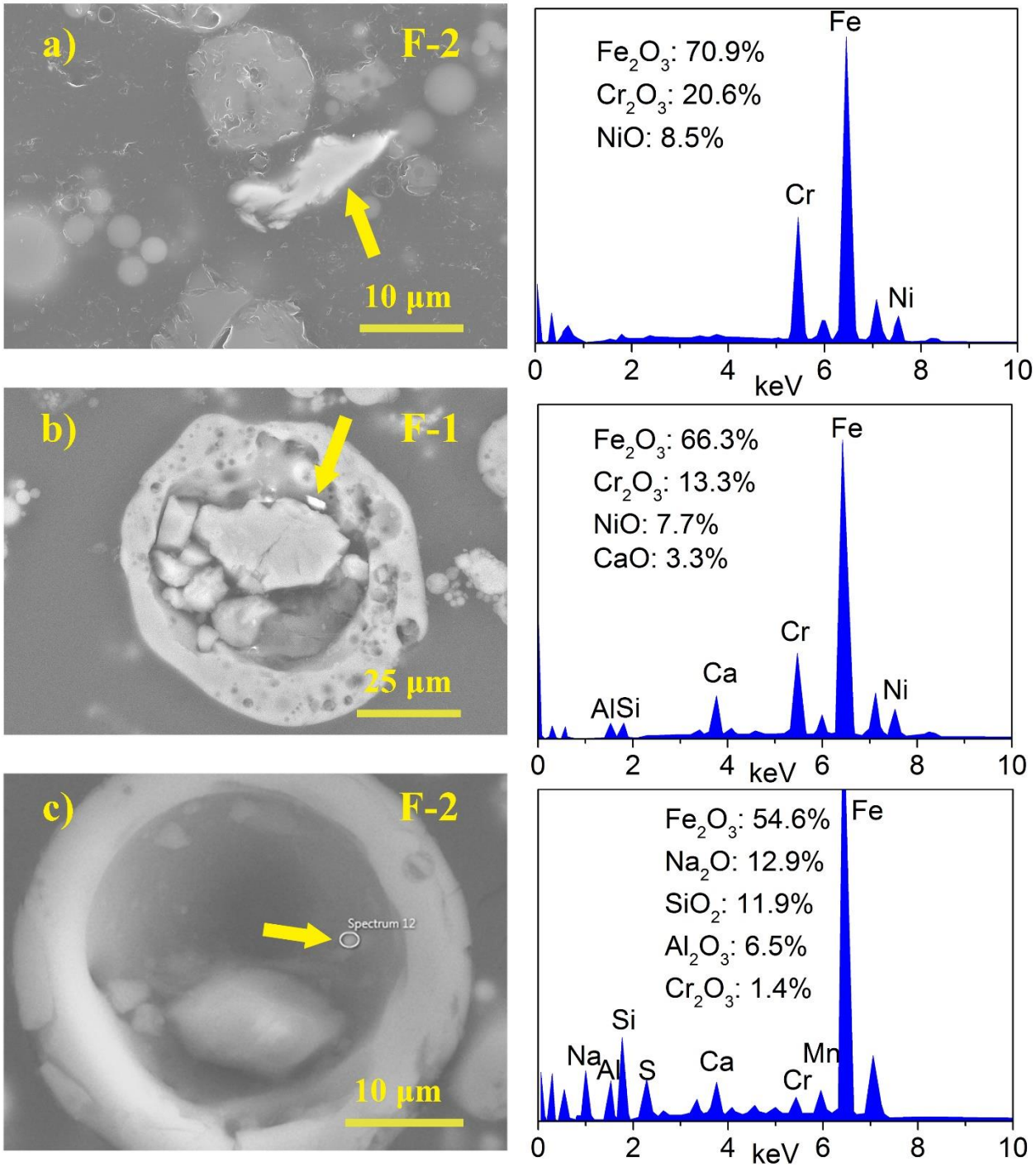


**Figure S3**. SEM images (left panels) and EDX spectra (right panels) showing Cr- and/or Ni-bearing phases in CFA samples (a) F-2, (b) F-1, and (c) F-2. Yellow arrows indicate particles for EDX measurements.

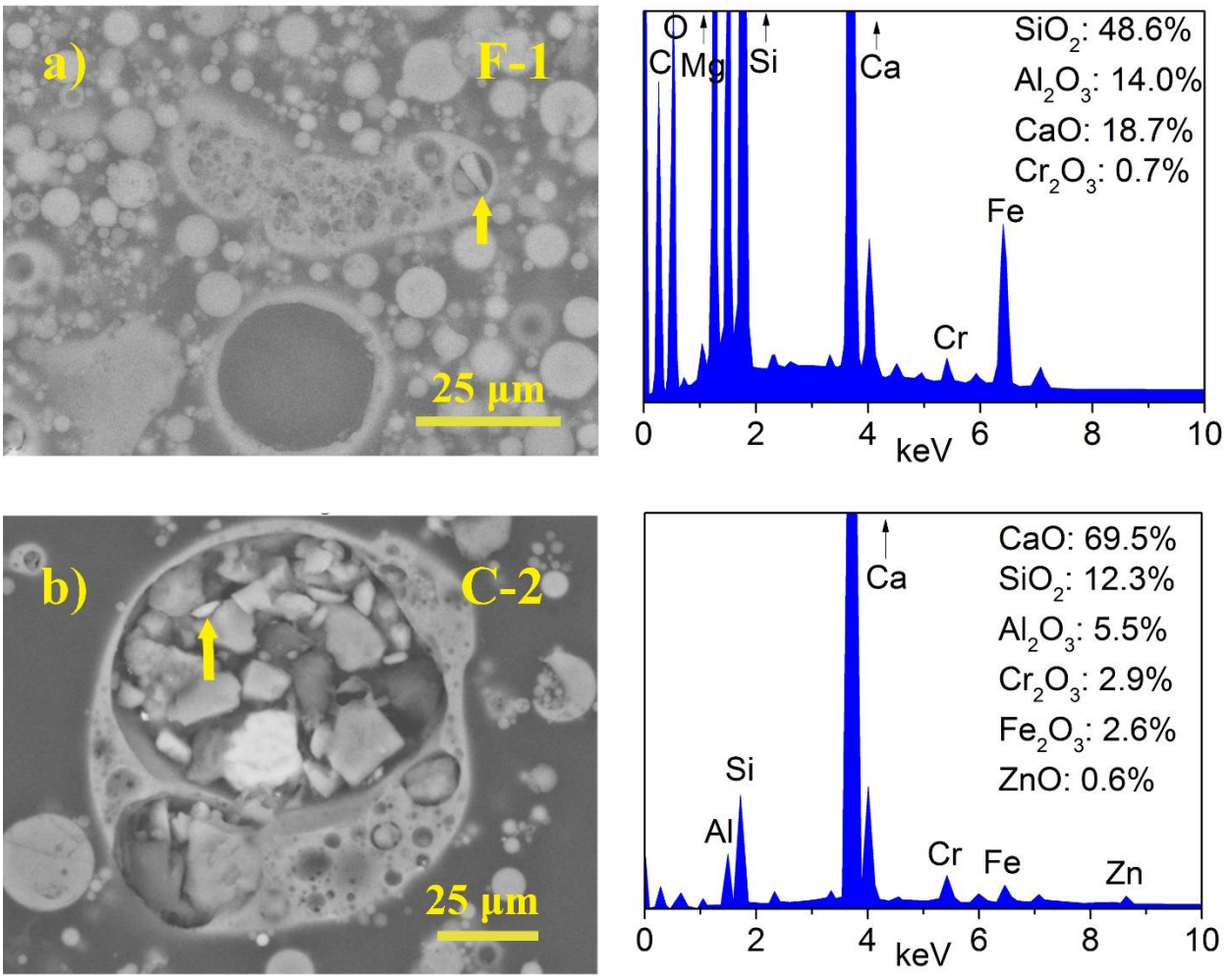


**Figure S4**. SEM images (left panels) and EDX spectra (right panels) showing Cr-bearing phases in CFA samples (a) F-1 and (b) C-2. Yellow arrows indicate particles for EDX measurements.

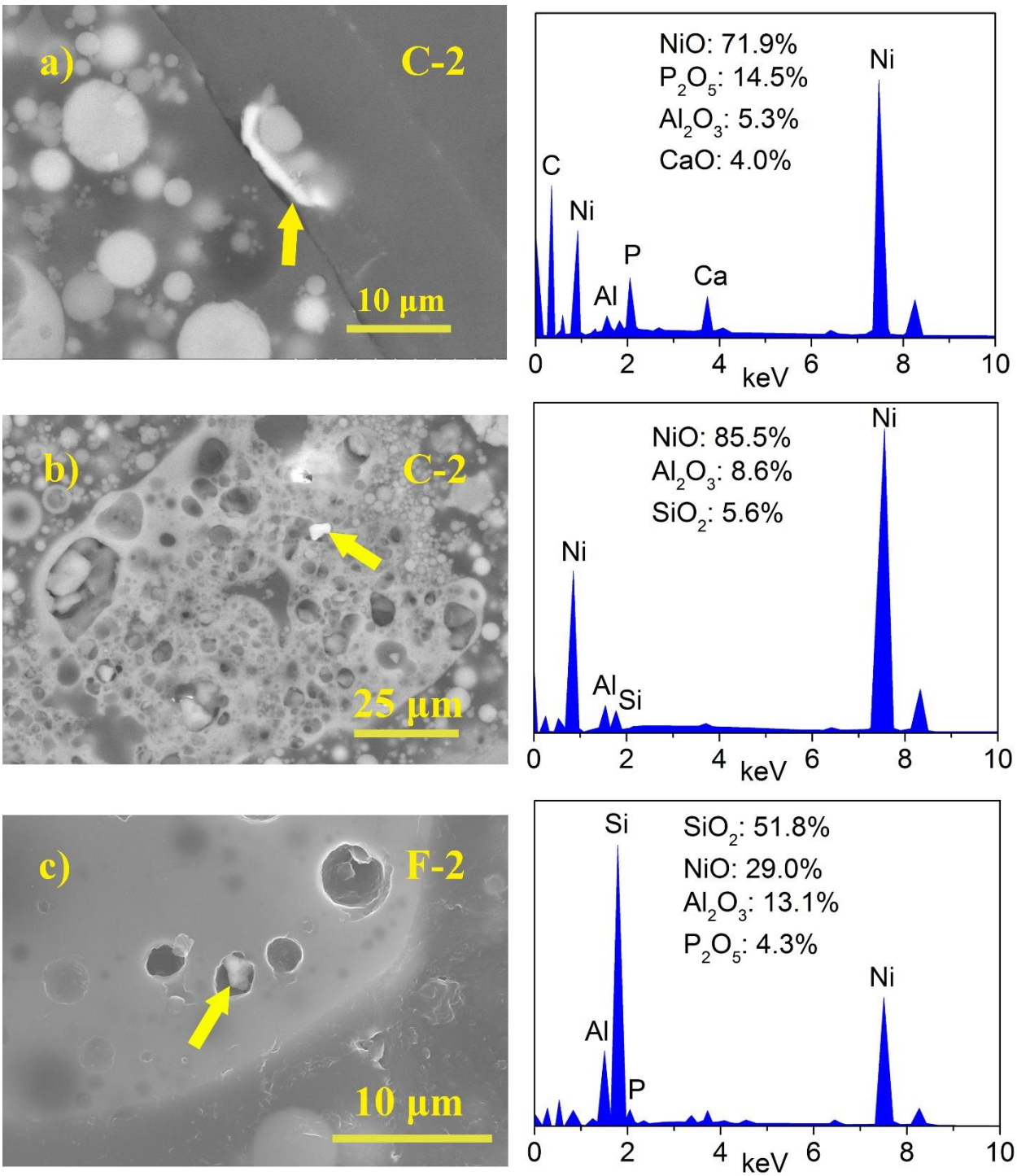


**Figure S5**. SEM images (left panels) and EDX spectra (right panels) showing Ni-bearing phases in CFA samples (a) C-2, (b) C-2, and (c) F-2. Yellow arrows indicate particles for EDX measurements.

**References**


Cornell RM, Schwertmann U. The iron oxides: structure, properties, reactions, occurrences and uses: John Wiley & Sons, 2003.

De Witte BM, Uytterhoeven JB. Acid and alkaline sol-gel synthesis of amorphous aluminosilicates, dry gel properties, and their use in probing sol phase reactions. Journal of colloid and interface science 1996; 181: 200-207.

Fu B, Liu G, Mian MM, Sun M, Wu D. Characteristics and speciation of heavy metals in fly ash and FGD gypsum from Chinese coal-fired power plants. Fuel 2019; 251: 593-602.

Jegadeesan G, Al-Abed SR, Pinto P. Influence of trace metal distribution on its leachability from coal fly ash. Fuel 2008; 87: 1887-1893.

Lin R, Stuckman M, Howard BH, Bank TL, Roth EA, Macala MK, et al. Application of sequential extraction and hydrothermal treatment for characterization and enrichment of rare earth elements from coal fly ash. Fuel 2018; 232: 124-133.

Liu P, Huang R, Tang Y. Comprehensive Understandings of Rare Earth Element (REE) Speciation in Coal Fly Ashes and Implication for REE Extractability. Environmental science & technology 2019; 53: 5369-5377.

McNear Jr DH, Chaney RL, Sparks DL. The effects of soil type and chemical treatment on nickel speciation in refinery enriched soils: A multi-technique investigation. Geochimica et Cosmochimica Acta 2007; 71: 2190-2208.

Pan J, Zhou C, Tang M, Cao S, Liu C, Zhang N, et al. Study on the modes of occurrence of rare earth elements in coal fly ash by statistics and a sequential chemical extraction procedure. Fuel 2019; 237: 555-565.

Quispe D, Pérez-López R, Silva LF, Nieto JM. Changes in mobility of hazardous elements during coal combustion in Santa Catarina power plant (Brazil). Fuel 2012; 94: 495-503.

Ravel B, Newville M. ATHENA, ARTEMIS, HEPHAESTUS: data analysis for X-ray absorption spectroscopy using IFEFFIT. Journal of synchrotron radiation 2005; 12: 537-541.

Saqib N, Bäckström M. Chemical association and mobility of trace elements in 13 different fuel incineration fly ashes. Fuel 2016; 165: 193-204.

Smeda A, Zyrnicki W. Application of sequential extraction and the ICP-AES method for study of the partitioning of metals in fly ashes. Microchemical Journal 2002; 72: 9-16.

Taggart RK, Rivera NA, Levard C, Ambrosi J-P, Borschneck D, Hower JC, et al. Differences in bulk and microscale yttrium speciation in coal combustion fly ash. Environmental Science: Processes & Impacts 2018; 20: 1390-1403.

Tang Y, Elzinga EJ, Lee YJ, Reeder RJ. Coprecipitation of chromate with calcite: batch experiments and X-ray absorption spectroscopy. Geochimica et Cosmochimica Acta 2007; 71: 1480-1493.

Tian Q, Guo B, Nakama S, Sasaki K. Distributions and leaching behaviors of toxic elements in fly ash. Acs Omega 2018; 3: 13055-13064.

Ure A, Quevauviller P, Muntau H, Griepink B. Speciation of heavy metals in soils and sediments. An account of the improvement and harmonization of extraction techniques undertaken under the auspices of the BCR of the Commission of the European Communities. International journal of environmental analytical chemistry 1993; 51: 135-151.

Winburn RS, Grier DG, McCarthy GJ, Peterson RB. Rietveld quantitative X-ray diffraction analysis of NIST fly ash standard reference materials. Powder Diffraction 2000; 15: 163-172.
Yan C, Li Q, Zhang X, Li G. Mobility and ecological risk assessment of heavy metals in surface sediments of Xiamen Bay and its adjacent areas, China. Environmental Earth Sciences 2010; 60: 1469-1479.
Yuan C-G. Leaching characteristics of metals in fly ash from coal-fired power plant by sequential extraction procedure. Microchimica Acta 2009; 165: 91-96.
Zeng L, Wan B, Huang R, Yan Y, Wang X, Tan W, et al. Catalytic oxidation of arsenite and reaction pathways on the surface of CuO nanoparticles at a wide range of pHs. Geochemical transactions 2018; 19: 12.
Zhao S, Duan Y, Lu J, Gupta R, Pudasainee D, Liu S, et al. Chemical speciation and leaching characteristics of hazardous trace elements in coal and fly ash from coal-fired power plants. Fuel 2018; 232: 463-469.